Oncogene (2001) 20, 34–47

www.nature.com/onc

Activation of ErbB-2 via a hierarchical interaction between ErbB-2 and type I insulin-like growth factor receptor in mammary tumor cells

Maria Eugenia Balañá[1], Leticia Labriola[1], Mariana Salatino[1], Federico Movsichoff[1], Giselle Peters[1], Eduardo H Charreau[1,2] and Patricia V Elizalde*[,1]

[1]*Instituto de Biología y Medicina Experimental (IBYME), Obligado 2490, Buenos Aires 1428, Argentina;* [2]*Facultad de Ciencias Exactas y Naturales, Universidad de Buenos Aires, Argentina*

The present study focused on interactions between signaling pathways activated by progestins and by type I and II receptor tyrosine kinases (RTKs) in mammary tumors. An experimental model in which the synthetic progestin medroxyprogesterone acetate (MPA) induced mammary adenocarcinomas in Balb/c mice was used. MPA-stimulated proliferation, both *in vivo* and *in vitro*, of progestin-dependent tumors induced up-regulation of ErbB-2 protein levels and tyrosine phosphorylation of this receptor. Combinations of antisense oligodeoxynucleotides (ASODNs) directed to ErbB-2 mRNA with ASODNs directed to the insulin-like growth factor-I receptor (IGF-IR) were used to study the effect of the simultaneous block of these receptors on the MPA-induced proliferation of epithelial cells from the progestin-dependent C4HD line. Neither synergistic nor additive effects on the inhibition of MPA-induced proliferation of C4HD cells were observed as a result of the combination of these ASODNs. Suppression of IGF-IR expression by ASODNs resulted in complete abrogation of MPA-induced phosphorylation of ErbB-2 in C4HD cells, whereas blockage of ErbB-2 did not affect IGF-IR phosphorylation. These results show the existence of a hierarchical interaction between IGF-IR and ErbB-2, by means of which IGF-IR directs ErbB-2 phosphorylation. We demonstrated, for the first time, that this hierarchical interaction involves physical association of both receptors, resulting in the formation of a heteromeric complex. Furthermore, confocal laser microscopy experiments demonstrated that MPA was able to induce co-localization of ErbB-2 and IGF-IR. This hetero-oligomer was also found in MCF-7 human breast cancer cells in which association of IGF-IR and ErbB-2 was induced by heregulin and IGF-I. *Oncogene* (2001) **20,** 34–47.

Keywords: ErbB receptors; mammary tumorigenesis; progestin; type I insulin-like growth factor receptor

Introduction

The positive role of estrogens in breast cancer development has long been acknowledged. Accumulated evidence has indicated that progestins are also involved in controlling mammary tumorigenesis (Kiss *et al*., 1986; Braunsberg *et al*., 1987; Manni *et al*., 1987; Clarke and Sutherland, 1990; Groshong *et al*., 1997; Lange *et al*., 1998). Although the mechanisms by which steroid hormones stimulate growth of breast cancer cells have not yet been completely deciphered, regulation of the expression of growth factors (GFs) which in turn act as mitogens for tumor cells, has already been proposed (Dickson and Lippman, 1995). Upon steroid hormones binding, estrogen (ER) and progesterone receptor (PR) act as nuclear transcription factors. On the other hand, most GFs bind to transmembrane receptors that carry an intrinsic activity of tyrosine kinase. Particularly, members of type I and II receptor tyrosine kinase families (RTKs) have been implicated in breast cancer development (Baserga, 1995, Pinkas-Kramaski *et al*., 1997). Type I RTKs includes four members: epidermal growth factor receptor (EGFR/ErbB-1) (Ullrich *et al*., 1984), ErbB-2 (Yamamoto *et al*., 1986), ErbB-3 (Kraus *et al*., 1989; Plowman *et al*., 1990), and ErbB-4 (Plowman *et al*., 1993). A direct consequence of ligand binding to the extracellular domain of type I RTKs is the formation of receptor dimers and stimulation of the intrinsic kinase activity, which leads to the phosphorylation of tyrosine residues in the intracellular domain of receptors (van der Geer *et al*., 1994). A large number of ligands for type I RTKs have been described. These include six ligands for EGF-R (Riese and Stern, 1998) and all isoforms of neu differentiation factor/heregulins (HRG) which bind to ErbB-3 and ErbB-4 (Tzahar *et al*., 1996). Interestingly, ErbB-2 is an orphan receptor. Despite the absence of a known ligand that binds ErbB-2 directly, this receptor participates in an extensive network of ligand-induced formation of ErbBs dimers (Graus-Porta *et al*., 1997).

Type II RTK family comprises the insulin receptor and the type I insulin-like growth factor receptor (IGF-IR) (LeRoith *et al*., 1995). Both are synthesized as a single peptide that is glycosylated and cleaved to an extracellular α chain and a transmembrane β chain. α and β chains are linked

*Correspondence: PV Elizalde
Received 6 June 2000; revised 19 October 2000; accepted 23 October 2000

by disulfide bonds to form an $\alpha\beta$-half receptor that is subsequently linked to another $\alpha\beta$-half receptor, by disulfide bonds between the α subunits, to form the mature α_2b_2-holoreceptor (LeRoith *et al*., 1995, Ullrich *et al*., 1986). Both insulin-like growth factors (IGFs)-I and -II bind to IGF-IR. The cytoplasmic portion of the β subunit contains the tyrosine kinase domain. Autophosphorylation on tyrosine residues in response to ligand binding to the extracellular α subunit occurs as an intramolecular trans-reaction, wherein the tyrosine kinase of one β-subunit phosphorylates residues located on the other β subunit of the tetrameric receptor (LeRoith *et al*., 1995, Ullrich *et al*., 1986).

Tyrosine residues in the intracellular domain of the RTKs, phosphorylated as a result of ligand binding, serve as docking sites for a number of SH2 and phosphotyrosine-binding (PTB) domain-containing proteins (Kavanaugh and Williams, 1994; Cohen *et al*., 1995) including the adaptor proteins SHC (Pelicci *et al*., 1992) and Grb2 (Lowenstein *et al*., 1992), which link RTKs to the mitogen activated protein kinase (MAPK) pathway (Egan and Weinberg, 1993), and the p85 subunit of the phosphatidyl inositol 3-kinase (PI-3K) (Fedi *et al*., 1994) that couples RTKs to the S6 kinase cascade (Ming *et al*., 1994). Interestingly, ErbB-3 which possesses the unique capacity among type I RTKs to bind and activate the p85 regulatory subunit of PI-3K (Carraway and Cantley, 1994; Fedi *et al*., 1994), provides a link between signal transduction pathways elicited through type I and II RTKs. Thus, activation of IGF-IR results in tyrosine phosphorylation of a substrate protein IRS-1, which in turn binds to and activates PI-3K (Backer *et al*., 1993).

Initially, signaling pathways were considered a linear way to transfer information. However, increasing evidence has clearly shown that signal transduction pathways interact with one another. These interactions result in quite complex networks with properties that the individual pathways lack. Accordingly, convergence between steroid hormones and GFs signaling pathways, that were previously thought to be separated pathways, has recently been shown. Estradiol stimulates Src kinase and the MAPK cascade in MCF-7 mammary tumor cells (Migliaccio *et al*., 1996). It is to be noted that progestins treatment of T47D breast cancer cells also results in the stimulation of the c-Src/$p21^{ras}$/MAPK transducing pathway (Migliaccio *et al*., 1998). The activation of this pathway by progestins not only requires the B isoform of the progesterone receptor, but also a ligand-free estrogen receptor (Migliaccio *et al*., 1998). Convergence between PR and GFs activated signaling pathways has also been demonstrated. Progestins treatment of T47D cells up-regulates ErbB-2 and ErbB-3 and enhances EGF-stimulated tyrosine phophorylation of signaling molecules known to associate with activated type I RTKs. It also potentiates EGF-stimulated p42/p44 MAPK, p38 MAPK and JNK activities (Lange *et al*., 1998, Richer *et al*., 1998). Independently of EGF, progestins increase Stat5 protein level and its association with phosphotyrosine-containing proteins (Lange *et al*., 1998, Richer *et al*., 1998)

The aim of the present study was to investigate interactions between progestins and RTKs signaling pathways by using the well characterized model of hormonal carcinogenesis in which the synthetic progestin medroxyprogesterone acetate (MPA) induces mammary adenocarcinomas in virgin female Balb/c mice (Molinolo *et al*., 1987; Lanari *et al*., 1989). Most of the MPA-induced tumors are of ductal origin, express high levels of ER and PR and are maintained by syngeneic transplants in MPA-treated mice, evidencing a progestin-dependent (HD) pattern of growth (Lanari *et al*., 1989). Tumor variants with an MPA-independent (HI) pattern of growth have been generated by transplantation into untreated mice. These HI tumors express the same ER and PR content as their parental HD counterparts (Lanari *et al*., 1989). Finally, MPA induces a small number of lobular mammary carcinomas which lack ER and PR expression and evidence an MPA-independent (HI) behavior (Molinolo *et al*., 1987; Lanari *et al*., 1989).

In the course of this study of the molecular mechanisms involved in cross-talk between RTKs and progestins, we found that a functional IGF-IR is required in order to phosphorylate and therefore activate ErbB-2. Thus, blocking IGF-IR expression by antisense oligodeoxynucleotides to its mRNA results in complete inhibition of MPA capacity to phosphorylate ErbB-2. The converse situation was not observed since blockage of ErbB-2 does not affect IGF-IR activation. These findings show a hierarchical interaction between IGF-IR and ErbB-2 in which IGF-IR directs ErbB-2 activation. Notably, and for the first time, we herein found the formation of a heteromeric complex between members of type I (ErbB-2) and II (IGF-IR) RTKs families. We also found that in the MCF-7 breast cancer cell line hetero-oligomerization of IGF-IR and ErbB-2 was induced by heregulin and IGF-I.

Results

Type I RTKs expression and activation in in vivo *progestin-dependent and -independent tumor lines and in primary cultures of epithelial cells*

We investigated the expression of type I RTKs in three types of tumors from the MPA-induced mammary tumor model. The first type were ductal progestin-dependent (HD) tumor lines C4HD and 53HD, that require MPA administration for their *in vivo* growth and express high levels of ER and PR (Molinolo *et al*., 1987; Lanari *et al*., 1989). The second were their progestin-independent (HI) variants C4HI and 53HI, that are able to grow in the absence of MPA administration. These HI tumors, in spite of an MPA-independent pattern of growth, retain ER and PR expression (Molinolo *et al*., 1987; Lanari *et al*.,

1989). The third type of tumors analysed were MPA-induced mammary carcinomas of lobular origin, 60, 39 and 55, that lack ER and PR expression and evidence a HI behavior (Molinolo *et al*., 1987; Lanari *et al*., 1989). ErbB-2, ErbB-3 and ErbB-4 proteins were expressed in all tumor lines examined (Figure 1a). As control for levels of ErbB-2 we used the human breast cancer MCF-7 cell line with low ErbB-2 content. C4HD and C4HI tumors evidenced significantly higher levels of ErbB-2 than MCF-7 cells (3–6-fold), comparable to those considered as overexpression in human breast cancer cell lines (Figure 1a) (Lupu and Lippman, 1993). In spite of the high ErbB-2 levels present in C4HD tumors, a significant increase (2–3-fold) of ErbB-2 expression was detected in C4HD tumors growing in MPA-treated mice, as compared with tumors growing in untreated animals (Figure 1a). C4HI variant exhibited ErbB-2 levels similar to those observed in C4HD tumors growing in MPA-treated mice (Figure 1a). Line 53HD showed levels of ErbB-2 comparable to those of MCF-7 cells (Figure 1a). MPA up-regulated ErbB-2 expression (3–4-fold) in 53HD tumors and the 53HI variant showed high levels of ErbB-2 (Figure 1a). HI lines of lobular histology 60, 39 and 55 expressed significantly higher levels of ErbB-2 than MCF-7 cells (4–6-fold), comparable with those present in C4HD tumors growing in MPA-treated mice (Figure 1a). As happened with ErbB-2, MPA induced an up-regulation of ErbB-3 in both C4 and 53 HD lines (4–6-fold) and the HI counterparts expressed levels similar to those of HD tumors growing in MPA-treated animals (Figure 1a). Furthermore, high levels of ErbB-3 in lobular HI lines 60, 39 and 55 were found (Figure 1a). Our analysis of ErbB-4 expression, using a panel of ErbB-4 specific antibodies, indicated the presence of low ErbB-4 in all three types of tumors (Figure 1a). MPA did not regulate its levels nor were there any differences in expression between HD tumors, their HI counterparts or HI tumors of lobular histology (Figure 1a).

We then investigated whether MPA was able to regulate the expression of type I RTKs in primary cultures of epithelial cells of the C4HD tumor line, selected as a model of a progestin-dependent pattern of growth. C4HD epithelial cells in culture proliferate very slowly in absence of MPA treatment, retain PR expression and the exquisite sensitivity to MPA stimulatory effect shown by the *in vivo* tumor line (Dran *et al*., 1995). We have previously reported that C4HD cells overexpress ErbB-2, contain high ErbB-3 protein levels and low ErbB-4 expression levels (Balañá *et al*., 1999). We are showing here that MPA treatment of C4HD cells resulted in the up-regulation of ErbB-2 and ErbB-3 levels, with no change in the low ErbB-4 levels (Figure 1b). The antiprogestin RU486, which inhibits MPA-induced proliferation of C4HD cells (Dran *et al*., 1995), abolished the capacity of MPA to induce ErbB-2 and ErbB-3 expression (Figure 1b). As a model of a progestin-independent (ER- and PR-) mammary cancer phenotype we selected lobular HI line 60. High levels of ErbB-2 and ErbB-3 expression were also observed in *in vitro* growth of 60 cells (Figure 1B). We had already found, by performing binding studies, that lobular HI tumors contained EGF-R (ErbB-1), while EGF-R presence was undetectable in ductal tumors (Kordon *et al*., 1994).

We then investigated the degree of tyrosine phosphorylation of ErbB-2 and ErbB-3 in *in vivo* tumor lines. Since MPA was able to up-regulate ErbB-2 and ErbB-3 levels, we first determined whether *in vivo* MPA proliferative effects were also associated with activation of the overexpressed ErbB-2 and ErbB-3 receptors. Therefore, extracts from C4HD tumors growing in MPA-treated and untreated mice were immunoprecipitated with anti-ErbB-2 or -ErbB-3 antibodies and the phosphotyrosine content of these receptors was

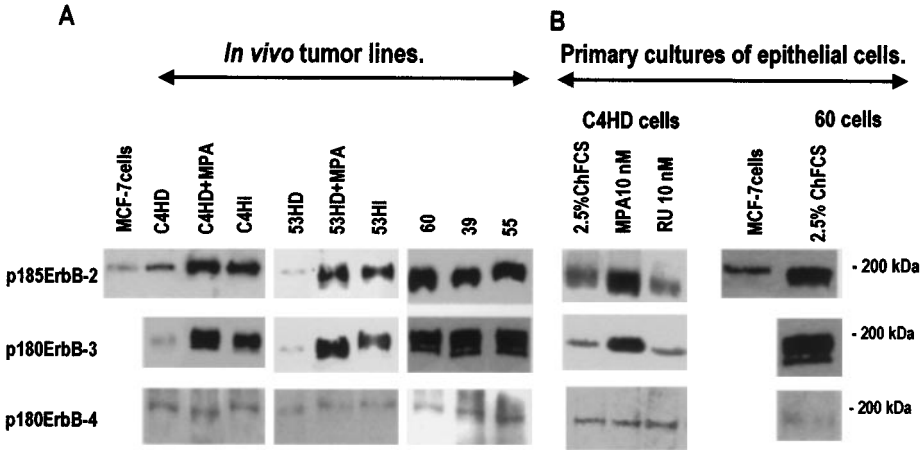

Figure 1 Expression of type I RTKs at protein level. (**a**) Eighty μg of protein from tumor lysates were electrophoresed and immunoblotted for ErbB-2, ErbB-3 and ErbB-4. MCF-7 human breast cancer cells were used as control for ErbB-2 expression levels. +MPA: tumors growing in MPA-treated mice. C4 and 53 are tumors from ductal origin; 60, 39 and 55 are progestin-independent tumors of lobular origin. (**b**) Primary cultures of epithelial cells from C4HD tumors were treated for 48 h with MPA 10 nM, MPA + RU486 (10 nM) or left untreated growing in 2.5% ChFCS, while 60 cells proliferated in 2.5% ChFCS. Eighty μg protein from cell lysates were electrophoresed and immunoblotted for ErbB-2, ErbB-3 and ErbB-4

determined by performing Western blotting with an anti-phosphotyrosine antibody. Figure 2 (a,c) shows that while low levels of tyrosine phosphorylation were observed in tumors growing in untreated mice, MPA induced a strong phosphorylation of both receptors. Progression of C4 ductal tumors to a HI phenotype was associated with a high degree of tyrosine phosphorylation of ErbB-2 and ErbB-3, comparable with the one observed in C4HD tumors growing in MPA-treated animals. Finally, autonomous proliferation of HI tumors 60 and 39 correlated with high levels of phosphorylation of ErbB-2 and ErbB-3 (Figure 2a, c). To verify that increased phosphorylation of ErbB-2 and ErB-3 in C4HD tumors growing in MPA-treated mice was due to an effect of MPA on the activation of these receptors, and not to the MPA-induced up-regulation of ErbBs levels, the amounts of protein immunoprecipitated from tumors growing in MPA-treated and untreated animals were different, in order to correct for the MPA-induced increase in ErbB-2 and ErbB-3 levels. Identical aliquots of immunoprecipitates were then subjected to immunoblot analysis with anti-ErbB-2 and ErbB-3 antibodies. Figure 2b,d show that almost equal amount of immunoprecipitated proteins were loaded, demonstrating that MPA is able to induce *in vivo* ErbB-2 and ErbB-3 phosphorylation. The same procedure, used to correct for different amounts of ErbBs expression, was performed to compare the degree of ErbB-2 and ErbB-3 phosphorylation between C4HD, C4HI, and HI lines of lobular histology 39 and 60 (Figure 2b,d).

We have recently determined that MPA treatment of primary cultures of C4HD epithelial cells during 48 h was able to induce a strong degree of ErbB-2 tyrosine phosphorylation (Balañá *et al*., 1999). In the present report we investigated whether the autonomous growth of 60 cells correlated with ErbB-2 tyrosine phosphorylation. As shown in Figure 2, in which C4HD cells are also included, 60 cells growing in 2.5% ChFCS evidence a high degree of constitutive phosphorylation of ErbB-2. The lower B panel shows that after the procedure used to correct for different ErbB-2 protein levels, nearly equal amounts of immunoprecipitated ErbB-2 were loaded.

Interaction between ErbB-2 and IGF-IR signaling pathways

We had previously found expression of IGF-IR, a member of type II RTKs family, and its ligand, namely IGF-I, in C4HD and 60 cells (Elizalde *et al*., 1990; 1998). MPA did not induce changes on IGF-IR or IGF-I expression in C4HD cells. In addition, levels of IGF-IR and IGF-I were similar in C4HD and 60 cell

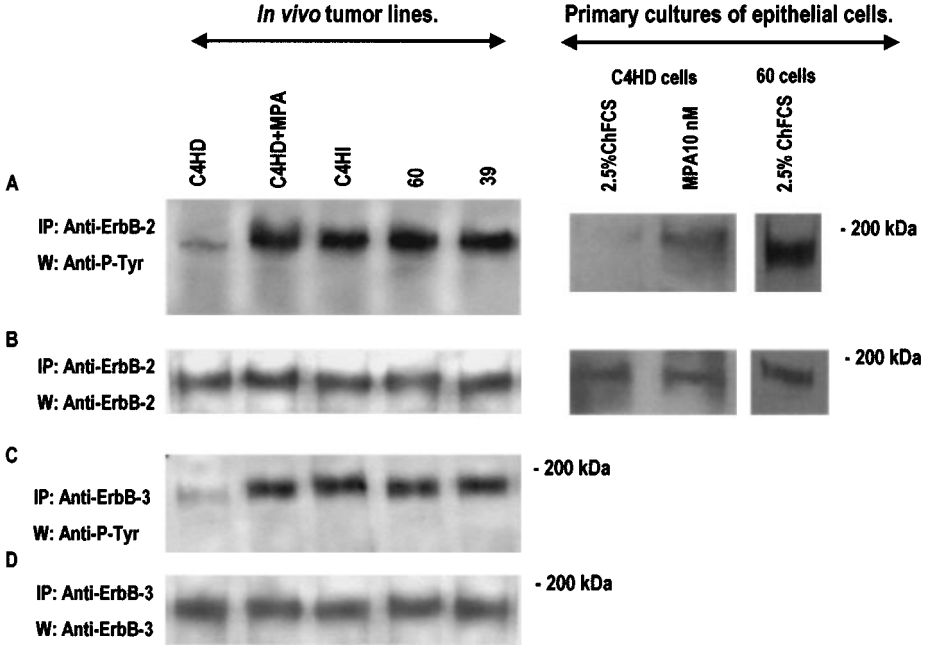

Figure 2 ErbB-2 and ErbB-3 tyrosine phosphorylation. (**a**) ErbB-2 and ErbB-3 were immunoprecipitated from tumor extracts and immunocomplexes were subjected to SDS–PAGE (7.5% gel) and analysed by Western blotting with an anti-P-Tyr mAb (**a** and **c**). In order to correct for the MPA-induced increase in ErbB-2 and ErbB-3 levels and for the higher expression of both receptors in HI lines, the amount of protein immunoprecipitated from tumors growing in MPA-treated and untreated animals and from HI tumors varied from 0.5–1.5 mg. Identical aliquots of each immunoprecipitate were subjected to immunoblot analysis with anti-ErbB-2 (**b**) or anti-ErbB-3 (**d**) antibodies to verify that nearly equal amount of immunoprecipitated proteins were loaded. +MPA: C4HD tumors growing in MPA-treated mice. (**b**) C4HD and 60 cells were lysed, ErbB-2 was immunoprecipitated from 0.5–1.5 mg of total proteins (in order to correct for the different level of expression as described in (**a**) and immunocomplexes were subjected to SDS–PAGE and analysed by Western blotting with an anti-P-Tyr mAb (upper panel). Identical aliquots of each immunoprecipitate were subjected to immunoblot analysis with anti-ErbB-2 antibody to verify that nearly equal amount of immunoprecipitated proteins were loaded (lower panel). W: Western blot, IP: immunoprecipitation

types (Elizalde *et al*., 1990; 1998). We also found that treatment of C4HD cells with antisense oligodeoxynucleotides (ASODNs) to IGF-IR resulted in a dose-dependent inhibition of MPA-mediated cell proliferation (Elizalde *et al*., 1998). On the other hand, recent findings in our laboratory demonstrated that incubation of C4HD cells with ASODNs to the translation start region of the ErbB-2 mRNA, also resulted in a dose-dependent inhibition of MPA-mediated proliferation (Balañá *et al*., 1999). These findings indicate that IGF-IR, activated by IGF-I, and ErbB-2, activated by HRG and MPA in C4HD cells (Balañá *et al*., 1999 and Figure 2) or constitutively activated in 60 cells (Figure 2), are involved in proliferative signaling pathways in both cell types. Thus, we investigated the potential antiproliferative effect of the simultaneous down-regulation ErbB-2 and IGF-IR. C4HD cells were treated with ASODN directed against IGF-IR and with ASODNs directed against ErbB-2. Figure 3a shows that while 1 μM of ASODNs to IGF-IR resulted

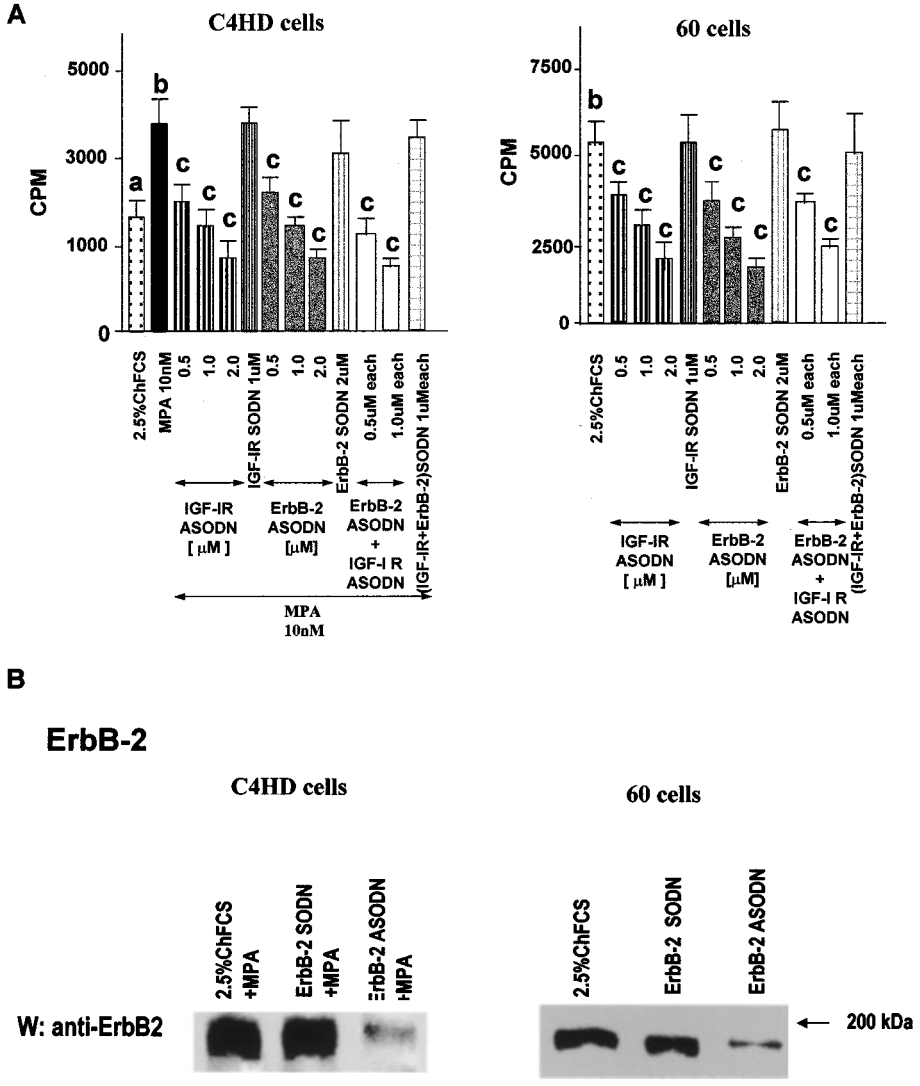

Figure 3 Effect of combinations of ErbB-2 ASODNS with IGF-IR ASODNS on C4HD and 60 cells growth. (**a**) Primary cultures of C4HD cells were incubated for 48 h in medium with 2.5% ChFCS supplemented with MPA 10 nM and MPA + ASODNs or SODNs to ErbB-2, IGF-IR or combinations of both, and 60 cells were incubated in medium with 2.5% ChFCS and treated with ASODNs as C4HD cells. Data are presented as mean $\pm$ sd. b *vs* a; c *vs* b: $P<0.001$. The experiments shown are representative of a total of eight for each cell type. (**b**) To study the effect of ErbB-2 ASODNs on protein synthesis 80 μg protein from C4HD and 60 cell lysates obtained from cells treated with 2 μM ErbB-2 ASODNs were electrophoresed and immunoblotted for ErbB-2. Densitometric analysis of ErbB-2 band expressed as percentage of the control value (i.e. C4HD cells growing in 10 nM MPA or 60 cells growing in 2.5% ChFCS) is: 28% for C4HD and 20% for 60 cells C4HD and 20% for 60 cells treated with 2 μM ASODN. No significant differences were found in densitometric values of ErbB-2 bands between control cells and cells treated with 2 μM SODN. Shown is a representative experiment of a total of eight for each cell type in which se was within 10%. The number of IGF-IR receptors in C4HD cells growing in MPA 10 nM or treated with 2 μM SODNs was 63.2 $\pm$ 4.8 fmol/mg protein, while in C4HD cells treated with 2 μM ASODNs the number was 15.2 $\pm$ 2.0 fmol/mg protein. In control or SODNs-treated 60 cells the number was 75.1 $\pm$ 6.4 fmol/mg protein, while in 60 cells treated with 2 μM ASODNs it was 18.6 $\pm$ 2.1 fmol/mg protein: Binding assays were performed as described in Materials and methods and data were analysed by Scatchard plot analysis (Scatchard, 1949)

in 47% of growth inhibition and 1 μM of ErbB-2 inhibited 52% of cell proliferation, combination of 1 μM ErbB-2 ASODNs with 1 μM IGF-IR ASODNs inhibited growth by 69%. This indicates lack of synergistic or additive effects between these ASODNs. We also tested combinations of ErbB-2 ASODNs and ASODNs to IGF-IR at lower doses, where antiproliferative effects were in the range of 35–45%. In C4HD cells a concentration of 0.5 μM IGF-IR ASODNs resulted in 42% of growth inhibition while 0.5 μM ErbB-2 ASODNs inhibited growth by 39% (Figure 3a). Combination of 0.5 μM of each resulted in inhibition of proliferation by 56% (Figure 3a). Similar results showing lack of additive effects were found when 60 cells were treated with combinations of ErbB-2 ASODNs and ASODNs against IGF-IR. For example, 1 μM IGF-IR ASODNs inhibited cell growth by 48%, 1 μM ErbB-2 ASODNs by 52% and the combination of 1 μM of each caused 60% growth inhibition (Figure 3a). These results support the notion that there may be an interplay between ErbB-2 and IGF-IR signaling pathways.

Blockage of IGF-IR expression by ASODNs results in inhibition of ErbB-2 tyrosine phosphorylation

We had previously reported that blockage of IGF-IR with ASODNs did not affect the levels of ErbB-2, ErbB-3 or ErbB-4 protein expression (Balañá *et al*., 1999). In addition, we found that blockage of ErbB-2 had no effect on ErbB-3 or ErbB-4 protein levels (Balañá *et al*., 1999). We are herein showing that ASODNs to ErbB-2 did not regulate IGF-IR content in C4HD and in 60 cells (Figure 4). Therefore, in order to elucidate whether interaction between ErbB-2 and IGF-IR could involve alterations in the activation of signaling pathways, we studied the level of tyrosine phosphorylation of ErbB-2 as a marker of its activation. As shown above, MPA treatment of C4HD cells resulted in the induction of ErbB-2 tyrosine phosphorylation and 60 cells displayed a strong degree of tyrosine phosphorylation (Figure 2). Therefore, primary cultures from both cell types were treated with IGF-IR ASODNs, protein extracts were immunoprecipitated with anti-ErbB-2 antibody and the phosphotyrosine content of ErbB-2 was determined by performing Western blotting with an anti-phosphotyrosine antibody. Figure 5 shows that phosphorylation of ErbB-2 was almost undetectable in C4HD cells treated with MPA plus IGF-IR ASODNs. ASODNs to IGF-IR (Figure 5) also abolished the constitutive tyrosine phosphorylation of ErbB-2 observed in 60 cells. We then explored the possibility that ErbB-2 ASODNs affected the phosphorylation of IGF-IR. C4HD and 60 cells were treated with ErbB-2 ASODNs and protein extracts were immunoprecipitated with an anti-phosphotyrosine antibody. Western was performed with an anti-IGF-IR β chain antibody. Tyrosine phosphorylation of IGF-IR β chain was readily detectable in MPA-treated C4HD cells and in 60 cells proliferating in ChFCS (Figure 5). This is due to the existence, in both cell types, of a functional autocrine loop, involving IGF-I and IGF-IR, that we have already described (Elizalde *et al*., 1990, 1998). As can be seen in Figure 5, blockage of ErbB-2 expression had no effect on the phosphorylation of the β chain of IGF-IR either in C4HD cells or in 60 cells. This experimental approach prevented us from using a similar strategy for control of IGF-IR loading than the one used for ErbB-2. Therefore, to demonstrate that the same levels of IGF-IR tyrosine phosphorylation corresponds to equivalent amounts of IGF-IR protein, we immunoprecipitated 1 mg protein from cells treated and untreated with ASODNs to ErbB-2, with an anti-IGF-IRα chain antibody and performed Western blot analysis with an anti-IGF-IRα chain antibody. As shown in Figure 5 equal amounts of IGF-IRα chain were present in cells treated and untreated with ASODNs. These filters were then stripped and reprobed with an antibody to the IGF-IRβ chain, showing that IGF-IRβ chain levels were equal in all protein extracts. Results shown in Figure 5 are consistent with the notion that the interaction between ErbB-2 and IGF-IR is not bidirectional but follows instead a hierarchy in which a functional IGF-IR is required in order to phosphorylate ErbB-2.

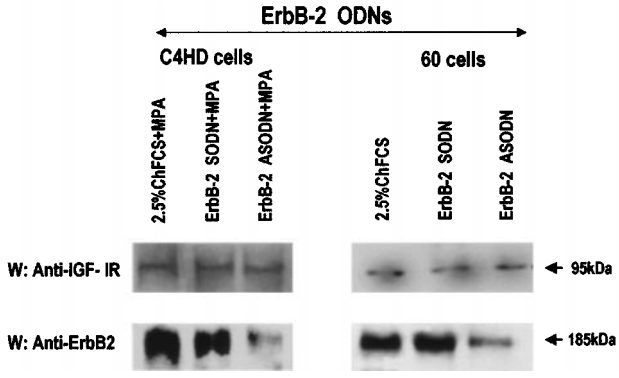

Figure 4 Effect of ErbB-2 ASODNs on IGF-IR expression. Cells were cultured in MPA 10 nM (C4HD) or 2.5% ChFCS (60) in presence or absence of ASODNs and SODNS to ErbB-2. One hundred μg protein from C4HD and 60 cell lysates were electrophoresed and immunoblotted for IGF-IR and ErbB-2. The experiment shown is representative of a total of four performed for each cell type

ErbB-2 and IGF-IR physically interact to form a heteromeric complex

We have recently reported that C4HD cells express HRG and that MPA increases HRG expression in these cells (Balañá *et al*., 1999). In addition, we found that HRG induced ErbB-2 phosphorylation in C4HD cells (Balañá *et al*., 1999). Therefore, we first evaluated whether IGF-IR could play an indirect role in ErbB-2 transactivation. This possibility implies that a functional IGF-IR could be required by MPA to induce HRG synthesis. We are herein showing that blockage of IGF-IR by ASODNs did not affect MPA capacity to induce HRG synthesis (Figure 6). This result

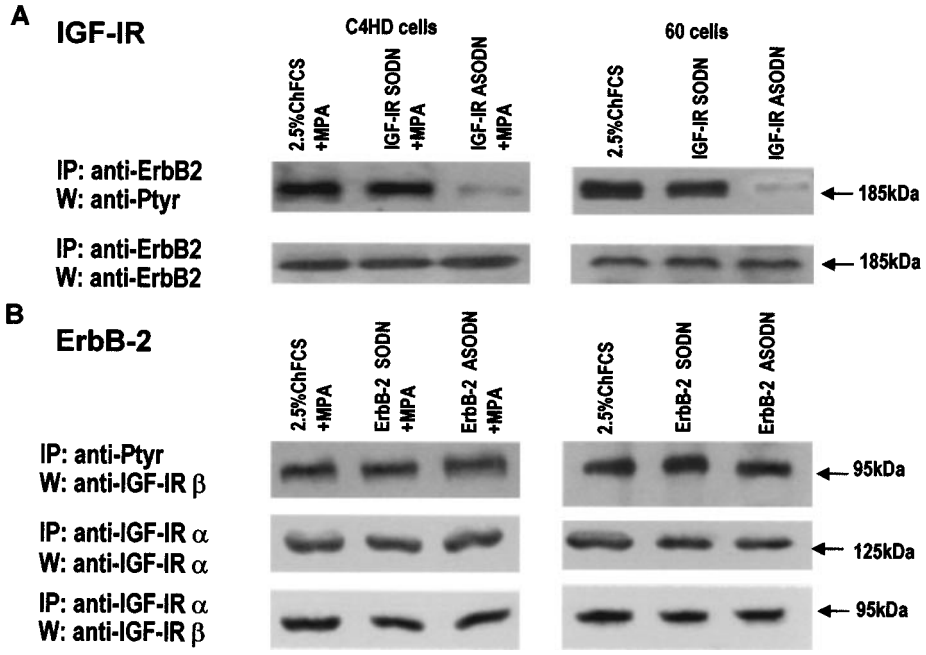

Figure 5 Blockage of IGF-IR inhibits ErbB-2 tyrosine phosphorylation but ASODNs to ErbB-2 have no effect on IGF-IR tyrosine phosphorylation. (**a**) C4HD cells cultured in MPA 10 nM and 60 cells growing in 2.5% ChFCS were treated with ASODNs and SODNS to IGF-IR. Cells were lysed, ErbB-2 was immunoprecipitated from 1 mg of total proteins and immunocomplexes were subjected to SDS–PAGE and analysed by Western blotting with an anti-P-Tyr mAb. Lower panel: Identical aliquots of each immunoprecipitate were subjected to immunoblot analysis with anti-ErbB-2 antibody to verify that nearly equal amount of immunoprecipitated proteins were loaded. (**b**) C4HD and 60 cells growing as described in (**a**) were treated with ErbB-2 ASODNs or SODNS. One mg protein from cell lysates was immunoprecipitated with an anti-P-Tyr mAb and immunocomplexes were analysed by Western blotting with an IGF-IR β chain antibody. Middle panel, one mg protein immunoprecipitated with an IGF-IR α chain antibody (Santa Cruz 2C8), was immunoblotted with an IGF-IR α chain antibody (Santa Cruz N-20). Lower panel, membranes shown in the middle panel were stripped and blotted with an IGF-IR β chain antibody. W: Western blot. IP: immunoprecipitation

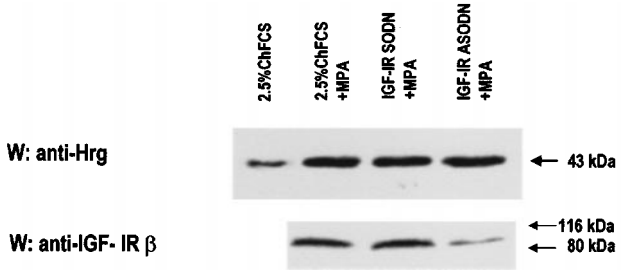

Figure 6 Blockage of IGF-IR does not affect MPA capacity to induce HRG synthesis. Primary cultures of C4HD cells were incubated for 48 h in 2.5% ChFCS, in 2.5% ChFCS supplemented with MPA 10 nM or with MPA + ASODNs or SODNs to IGF-IR mRNA. One hundred μg protein from cell lysates were electrophoresed and immunoblotted for HRG. The experiment shown is representative of a total of three. Lower panel shows the inhibition of IGF-IR expression in C4HD cells treated with IGF-IR ASODNs

suggests that IGF-IR role in ErbB-2 transactivation could be due to a direct interaction between both receptors. Further support to this hypothesis was provided by the fact that blockage of IGF-IR in 60 cells that do not express HRG (Balañá *et al*., 1999) resulted in the complete abrogation of ErbB-2 constitutive phosphorylation. Although the existence of heterodimerizations between members of type I RTKs family has been well documented, the formation of complexes between members of different RTKs has not been reported. In an attempt to define more precisely the interaction between ErbB-2 and IGF-IR, we studied the probable association between these two receptors. Membrane preparations, obtained in non-reducing conditions from C4HD tumors growing in MPA-treated and untreated mice and from 60 tumors, were immunoprecipitated with an anti-ErbB-2 antibody and were blotted separately with antibodies to the α and the β chain of IGF-IR. Same procedure was followed with protein extracts obtained from primary cultures of C4HD and 60 cells. As shown in Figure 7a co-immunoprecipitation of ErbB-2 with the α chain (upper panel) and with the β chain (middle panel) of IGF-IR was found in both C4HD and 60 *in vivo* tumors and in C4HD and 60 cells. Furthermore, an increase in the abundance of this complex was induced *in vivo* by MPA in C4HD tumors, in accordance with the increase in ErbB-2 levels induced by MPA in C4HD tumors (Figure 7a, lower panel). MPA treatment of C4HD cells during 48 h induced also a threefold increase in the abundance of the complex between ErbB-2 and IGF-IR α and β subunits (Figure 7a, upper and middle panel). Increase in the levels of this heteromeric complex in cells treated with MPA correlates with MPA-up regulation of ErbB-2 content

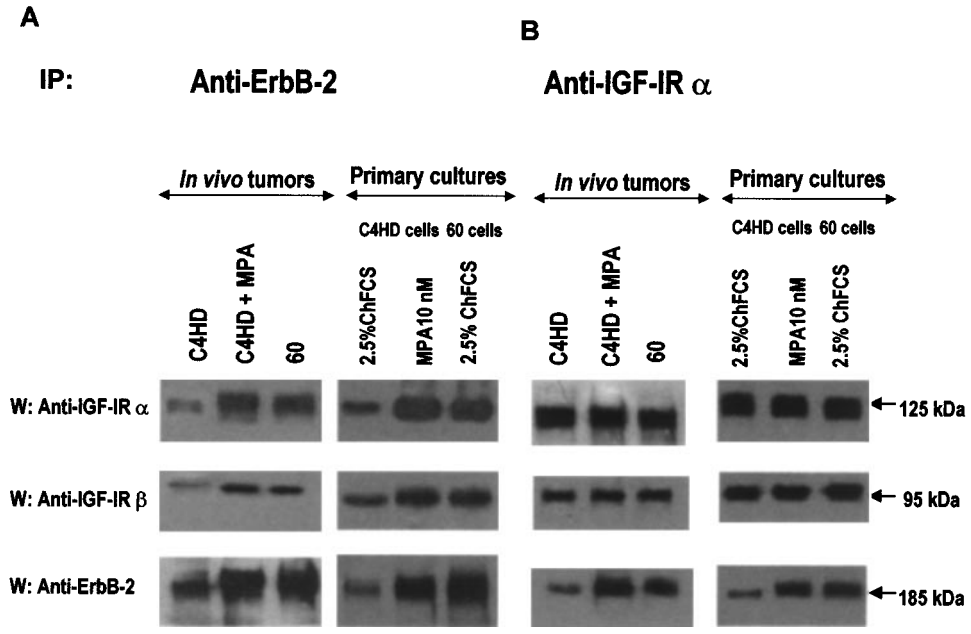

Figure 7 Binary complex between ErbB-2 and IGF-IR. Membrane preparations of C4HD tumors growing in MPA-treated (+MPA) and untreated mice and from 60 tumors were obtained in non-reducing conditions. Protein extracts from C4HD and 60 cells were obtained as described in Materials and methods. ErbB-2 (**a**) and IGF-IR α subunit (**b**) were immunoprecipitated from 1 mg membrane protein and immunocomplexes were subjected to SDS–PAGE (7.5% gel) and analysed by Western blotting with an anti-IGF-IR α subnunit (upper panel), an anti-IGF-IR β subunit (middle panel) and an anti-ErbB-2 antibody (lower panel)

(Figure 7a, lower panel). Interaction between ErbB-2 and IGF-IR was also detected when the immunoprecipitation-immunoblotting procedure was reversed. When membrane preparations or cell extracts were immunoprecipitated with an anti-IGF-IR α chain antibody and Western blotting was performed with an anti-ErbB-2 antibody, a clear association between ErbB-2 and IGF-IR α was found (Figure 7b, lower panel). As expected, when IGF-IR α chain immunoprecipitates were blotted with β chain of the receptor, association between α and β chains was evident (Figure 7b, middle panel). In an attempt to gain information about preferential association between ErbB-2 and IGF-IR α or β chains, we reduced the disulfide bridge that binds α and β subunits by using DTT in membrane preparations. However, when we immunoprecipitated membranes, obtained under reducing conditions, with the IGF-IR α chain and performed Western blotting with the IGF-IR β chain antibody, association between α and β chains of the receptor was found, probably due to the close interaction of the chains in the tetrameric receptor (data not shown). This fact prevented us from further defining sites of ErbB-2 and IGF-IR interaction.

Specificity of the interaction between ErbB-2 and IGF-IR was demonstrated by several experimental approaches. Shown are the results obtained using C4HD cells growing in MPA 10 nM. First, normal rabbit serum failed to immunoprecipitate ErbB-2 (Figure 8) and immune complexes of normal mouse serum did not contain IGF-IR α or β protein (Figure 8). Immunoprecipitation of ErbB-2 in the presence of a blocking peptide was also used as control (Figure

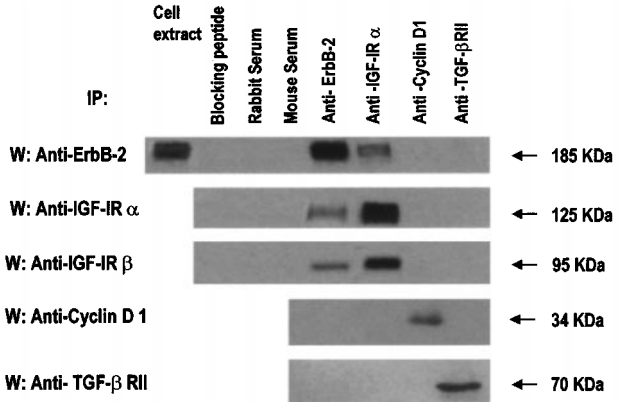

Figure 8 Specificity of the interaction between ErbB-2 and IGF-IR. Protein extracts (1 mg) from C4HD cells treated with MPA 10 nM were immunoprecipitated with the indicated antibodies. As controls, ErbB-2 was immunoprecipitated in presence of an ErbB-2 blocking peptide and protein extracts were incubated with pre-immune mouse or rabbit serum. One hundred μg protein of cell extract was directly immunoblotted with the ErbB-2 antibody (first lane, upper panel). W: Western blotting, performed with the indicated antibodies

8). Second, to control against the possibility that ErbB-2 and IGF-IR bind nonspecificically with a number of cellular proteins, two different proteins were tested. We chose another cell surface receptor, the transforming growth factor β receptor type II (TGF-βRII), which belongs to the family of transmembrane serine/threonine kinases, and cyclin D1, a protein involved in cell cycle control in the nucleus. Figure 8 shows that neither cyclin D1 nor

TGF-βRII bands were present when cell extracts were immunoprecipitated with ErbB-2 or IGF-IRα. Same results were obtained by the converse immunoprecipitation-immunoblotting procedure. Cyclin D1 or TGF-βRII immunoprecipitates contained no ErbB-2 or IGF-IR α or β bands (Figure 8). These data indicate that ErbB-2 and IGF-IR are not interacting promiscuously with other cellular proteins, including other transmembrane receptors or a protein that exerts its function in the nucleus. We also found that a significant amount of ErbB-2 (approximately 6%) was associated with IGF-IR (Figure 8). Further support for the existence of an association between ErbB-2 and IGF-IR in intact cells was provided by immunofluorescence confocal microscopy. C4HD cells were cultured in absence and presence of MPA 10 nM for 48 h. The analysis of immunostained cells showed that ErbB-2 and IGF-IR were distributed homogeneously on the cell surface of C4HD cells (Figure 9, left and middle panels, first and second row). When the relative localization of both receptors was determined by superimposing the two images (Figure 9, right panels, first and second row), MPA was found to induce an extensive co-localization of ErbB-2 (red) and IGF-IR (green) yielding a yellow fluorescence signal (Figure 9 right panel, second row).

The model system in which we have determined the existence of an association between IGF-IR and ErbB-2 is rather complex taking into account that IGF-IR is activated through an autocrine mechanism by endogenously produced IGF-I while ErbB-2 is activated by both endogenous HRG and MPA (Balañá *et al*., 1999 and Figure 2). Thus, we investigated whether this hetero-oligomer is present in MCF-7 cells that provide a simpler experimental model. MCF-7 cells express IGF-IR and ErbB-2 but not the ligands for these receptors, IGF-I and HRG (Stewart *et al*., 1990; Holmes *et al*., 1992; Lewis *et al*., 1996). As has been well acknowledged exogenously added IGF-I and HRG stimulate MCF-7 cells proliferation (Stewart *et al*., 1990; Holmes *et al*., 1992; Lewis *et al*., 1996). Thus, we herein investigated whether these ligands could induce association of IGF-IR and ErbB-2. MCF-7 cells growing in 0.1% serum were treated with IGF-I or HRG for 10, 30 min and 6 h, and protein extracts were immunoprecipitated with an anti-ErbB-2 antibody and were blotted with an antibody to the α chain of IGF-IR. As shown in Figure 10 while barely detectable association between IGF-IR and ErbB-2 was found in cells growing in 0.1% serum, both HRG and IGF-I were able to induce the formation of a heteromeric complex between IGF-IR and ErbB-2. The amount of complex was maximal after 10 min of HRG or IGF-I treatment, remained high at 30 min and decreased significantly after 6 h of HRG or IGF-I stimulation. Interaction between ErbB-2 and IGF-IR was also detected reversing the immunoprecipitation-immunoblotting procedure. As can be seen in Figure 10, a clear association between ErbB-2 and IGF-IR α induced by HRG and IGF-I was found when protein extracts were immunoprecipitated with an anti-IGF-IR α chain antibody and Western blotting was performed with an anti-ErbB-2 antibody.

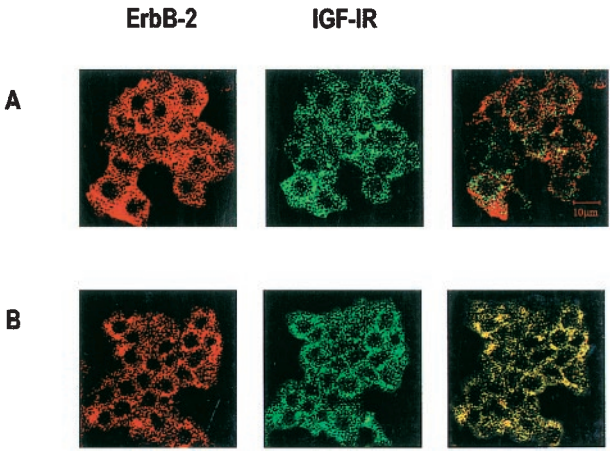

Figure 9 Localization of ErbB-2 and IGF-IR by immunofluorescence and confocal microscopy. C4HD cells were incubated in 2.5% ChFCS in absence (**a**) or presence of MPA (**b**) for 48 h at 37°C. ErbB-2 was localized using an ErbB-2 rabbit polyclonal antibody followed by incubation with rhodamine-conjugated anti-rabbit secondary antibody (red). IGF-IR was localized using an IGF-IR mouse monoclonal antibody followed by incubation with a FITC-conjugated anti-mouse secondary antibody (green). The same cells are shown in each row and images in the right panel are formed by superimposition of images from the other two panels in the same row. MPA induced co-localization of ErbB-2 and IGF-IR denoted by yellow colour (co-localization of red and green staining) on the cell surface. Representative of three experiments. Scale bars, 10 μm

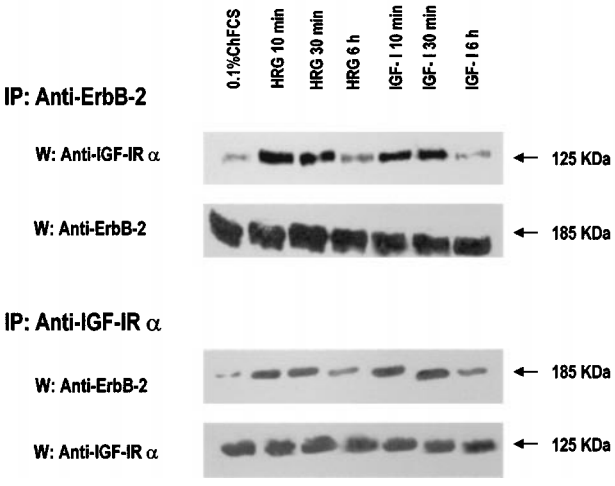

Figure 10 Binary complex between ErbB-2 and IGF-IR induced by HRG and IGF-I in MCF-7 cells. Protein extracts (1 mg) from MCF-7 cells growing in 0.1% ChFCS and treated with HRG (20 ng/ml) or IGF-I (50 ng/ml) were immunoprecipitated with anti-ErbB-2 or anti-IGF-IR α subunit antibodies. Immunocomplexes were subjected to SDS–PAGE (7.5% gel) and analysed by Western blotting with the indicated antibodies

Discussion

Our data show a new network of interactions among signal transduction pathways activated by PR and by members of type I (ErbB-2) and II (IGF-IR) receptor tyrosine kinase families, in a model system in which progestins induce both *in vivo* and *in vitro* proliferation of mammary tumor cells (Molinolo *et al*., 1987; Lanari *et al*., 1989). One of the most important aspects of the present work is that we have been able to demonstrate the existence of a hierarchical interaction between type I IGF-R and ErbB-2 by means of which IGF-IR directs ErbB-2 activation.

MPA induces ErbB-2 and ErbB-3 expression and tyrosine phosphorylation through binding to the progesterone receptor

ErbB-2, ErbB-3 and ErbB-4 expressions were found in *in vivo* lines of the MPA-induced mammary tumor model in Balb/c mice. Our present findings have demonstrated that MPA *in vivo* treatment of progestin-dependent ductal tumors was able to induce both expression and tyrosine phosphorylation and therefore activation of ErbB-2 and ErbB-3. Progestin-independent growth of both ductal and lobular tumors was associated with high levels of expression and tyrosine phosphorylation of these receptors, suggesting that in the steroid-independent growth of these tumors, control of proliferation is transferred from progestins biochemical pathways to signaling cascades in which ErbB receptors are involved. MPA was also able to up-regulate ErbB-2 and ErbB-3 expressions and to induce ErbB-2 tyrosine phosphorylation on primary cultures of epithelial cells from C4HD tumors. In addition, the antiprogestin RU486 inhibited MPA induction of ErbB-2 and ErbB-3 expression, indicating that MPA exerts this effect through binding to the PR.

Multiple factors and levels of regulation are involved in controlling ErbB-2 expression on breast tumors. Particularly, hormonal modulation of ErbB-2 expression has been described. Thus, several laboratories have clearly established that estrogens down-regulate ErbB-2 expression at mRNA and protein levels and that this effect is reversed by antiestrogens (Dati *et al*., 1990; Read *et al*., 1990; Taverna *et al*., 1994; Grunt *et al*., 1995; De Bortoli and Dati, 1997). Although interactions between EGF-R and progestins have been described (Murphy *et al*., 1986, 1988; Sarup *et al*., 1988), progestins effects on ErbB-2 expression remain less elucidated. Taverna *et al*. (1994) reported that in culture conditions where progestin inhibited cell growth of the breast tumor cell lines T47D and ZR75.1, progesterone caused an up-regulation of ErbB-2 at mRNA and protein level. Progesterone was found to increase EGF-R and ErbB-2 phosphorylation in the feline mammary adenocarcinoma line K12, although it was not able to sustain cell growth (Modiano *et al*., 1991). In contrast, other authors reported no effect on ErbB-2 mRNA or protein expression by progestins or antiprogestins treatment of MCF-7 cells primed with estradiol, that contains high levels of PR, and of T47D cells with high PR content. However, the authors did not describe progestins or antiprogestins effects on the proliferation of these cells (Read *et al*., 1990). Our present findings agree with those recently reported by Lange *et al*., (1998) in that the progestin R5020 up-regulated ErbB-2 and ErbB-3 expression in breast cancer cell line T47DYB, which constitutively expresses the B isoform of PR. However, a remarkable difference between these findings and ours is that Lange *et al*. (1998) found that up-regulation of ErbB-2 and ErbB-3 after R5020 treatment occurs under conditions in which R5020 inhibits T47DYB cells proliferation. These authors (Lange *et al*., 1998) also demonstrated that up regulation of ErbB-2 and ErbB-3 by R5020, during the progestin-arrested state of the cells, resulted in the potentiation of EGF-stimulated signaling pathways. Thus, R5020 enhanced EGF-induced tyrosine phosphorylation of EGF-R and of signaling molecules that associate with activated RTKs type I, such as Cbl and the p66 and p52 Shc isoforms. Notably, our research is the first to find that progestin-induced proliferation of mammary cancer cells involves up-regulation and activation of ErbB-2 and ErbB-3, providing a link between progestin stimulation of growth and ErbBs signaling pathways. As regards to ErbB-4, Lange *et al*. (1998) reported that in T47DYB cells, its levels were low and remained unchanged by progestin treatment, as we have also found in the present work.

Activation of ErbB-2 via a hierarchical interaction with IGF-IR

The link between signal transduction pathways elicited through type I and II RTKs is provided by ErbB-3 which possesses the unique capacity among type I RTKs to bind and activate the p85 regulatory subunit of PI-3K (Carraway and Cantley, 1994, Fedi *et al*., 1994, Graus-Porta *et al*., 1997). This ability to associate with PI-3K confers ErbB-3 the capacity of sharing signal transducction pathways with IGFs, since activation of IGF-IR results in tyrosine phosphorylation of a substrate protein IRS-1, which in turn binds to and activates p85 (Backer *et al*., 1993). The existence of interactions between ErbB-2 and IGF-IR signaling pathways in mammary tumor cells, has been a consistent finding in our laboratory. We have recently reported that C4HD cells cannot respond to HRG with mitogenesis in the absence of a functional IGF-IR (Balañá *et al*., 1999). In the course of the present work, the existence of interactions between ErbB-2 and IGF-IR was suggested by the finding that combinations of ASODNs directed against ErbB-2 and against IGF-IR showed lack of synergistic or additive effects. Additive effects could have been expected if IGF-IR and ErbB-2 targeted different independent signaling pathways. Synergistic interaction could have been existed if one receptor pathway potentiated or enhanced the other receptor biochemical pathway. Thus, only a mechanism

involving a hierarchical interaction between IGF-IR and ErbB-2, wherein one of the receptors is essential for the activation of signal transduction pathways elicited by the other, could fit our results. In fact, we demonstrated herein that abolishing IGF-IR expression resulted in the inhibition of MPA-induced phosphorylation of ErbB-2, in C4HD cells, and in inhibition of the constitutive tyrosine phosphorylation of ErbB-2 in 60 cells. Since abolishing ErbB-2 expression had no effect on IGF-IR tyrosine phosphorylation, our findings demonstrate that there is actually a hierarchical interaction between these receptors and that a functional IGF-IR is required in order to phosphorylate and thus activate ErbB-2. Several reports have previously shown the involvement of IGF-IR in ErbBs signaling pathways. Thus, mouse embryo fibroblasts overexpressing ErbB-2 but lacking IGF-IR do not respond to EGF-induced mitogenesis or transformation (Coppola *et al*., 1994) and prolonged activation of ERK2 by EGF in mouse embryo fibroblasts requires a functional IGF-IR (Swantek and Baserga, 1999). Interaction between type I and II RTKs has also been observed in mammary epithelial cells. Ethier and his co-workers demonstrated the existence of synergistic interactions between EGF-R and IGF-IR in normal mammary epithelial cells which show an absolute requirement of the simultaneous stimulation of both receptors to proliferate (Ram *et al*., 1995). Links between ErbB-2 and IGF-IR have also been reported in breast cancer. Thus, in the 21T series of breast cancer cell lines, progressive increase in ErbB-2 levels and constitutive tyrosine phosphorylation correlated with IGF-I independence in the 21MT-2 cells, with intermediate ErbB-2 levels, and with combined IGF-I and EGF independence in the 21MT-1 variant which expresses very high levels of activated ErbB-2 (Ram *et al*., 1996). Recently, ErbB-2 was transducted into the normal human mammary epithelial cells MCF-10A and H16N2 (Woods Ignatoski *et al*., 1999). ErbB-2 overexpression confers to both cell lines insulin growth independence. Our own results demonstrating that a functional IGF-IR is required in order to phosphorylate and then activate ErbB-2 are in line with all these findings. Thus, it may be interpreted that since IGF-IR is required to activate ErbB-2, cells expressing very high levels of constitutively activated ErbB-2 do not require a functional IGF-IR to proliferate. Therefore, these cells become independent of IGFs to proliferate.

The unorthodox cross-talk between type I and II RTKs family members, described herein for the first time, involves a physical association between ErbB-2 and IGF-IR, directly or indirectly via an additional component. We found using both immunoprecipitation and confocal microscopy that MPA is able to increase the levels of this heteromeric complex in C4HD cells, in parallel with its ability to induce up-regulation of ErbB-2. The presence of the ErbB-2/IGF-IR complex was also found in progestin-independent 60 cells which overexpress ErbB-2, indicating that physical association with IGF-IR is a general mechanism of ErbB-2 activation in both hormone-dependent and -independent mammary tumor cells. Further evidence indicating that association between ErbB-2 and IGF-IR is a molecular mechanism that occurs in the signaling pathways of these receptors was provided by our findings in MCF-7 breast cancer cells. In these cells, IGF-I and HRG were able to induce hetero-oligomerization of ErbB-2 and IGF-IR, in parallel to their capacity to stimulate MCF-7 cell growth.

As a whole, our results are consistent with an entirely new model to explain the molecular mechanisms underlying ErbB-2 activation. Currently, since ErbB-2 is an orphan receptor, its activation has been explained by the formation of an extensive network of dimers with the other type I RTKs, induced by the ligands of EGF-R, ErbB-3 and ErbB-4 (Graus-Porta *et al*., 1997). We now show that ErbB-2 is able to form a heteromeric complex with IGF-IR, a type II RTK. The hierarchical importance of IGF-IR in the process of ErbB-2 activation is demonstrated by our finding that in absence of a functional IGF-IR, ErbB-2 does not become phosphorylated even when the expression of the known heterodimeric partners of ErbB-2, namely EGF-R, ErbB-3 and ErbB4, is not affected by the lack of IGF-IR. It remains to be elucidated whether a different set of tyrosine residues are phosphorylated within the ErbB-2 molecule after ErbB-2 dimerization with the other type I RTKs, than those which result phosphorylated when ErbB-2 physically associates with IGF-IR and whether phosphorylation of both sets of residues is required in order to link ErbB-2 activation with mitogenic signaling pathways.

Materials and methods

Animals and tumors

Experiments were carried out in virgin female Balb/c mice raised at the National Academy of Medicine of Buenos Aires. All animal studies were conducted in accordance with the highest standards of animal care as outlined in the NIH guide for the Care and Use of Laboratory Animals. Hormone-dependent ductal tumors (C4HD and 53HD) originated in mice treated with 40 mg MPA every 3 months for 1 year and have been maintained by serial transplantation in animals treated with 40 mg sc MPA depot on the opposite flank to tumor inoculum (Molinolo *et al*., 1987; Lanari *et al*., 1989). Their hormone independent counterparts, C4HI and 53HI developed from HD tumors growing in mice that were not treated with MPA, approximately a year after the inoculum (Molinolo *et al*., 1987; Lanari *et al*., 1989). These HI tumor lines have been maintained by serial transplantation in untreated female mice. Tumor lines C4HD and 53HD are of ductal origin and express PR and ER (Molinolo *et al*., 1997; Lanari *et al*., 1989). Although their respective HI counterparts C4HI and 53HI have developed the capacity to grow in the absence of progestin treatment, they have retained PR and ER (Molinolo *et al*., 1997; Lanari *et al*., 1989). HI lines 60, 39 and 55 originated in MPA-treated mice and have been maintained by syngeneic transplants in

untreated virgin female mice. They are of lobular origin and express EGF-R but not PR or ER (Lanari *et al*., 1989).

Primary cultures and cell proliferation assays

Primary cultures of epithelial cells from C4HD tumors, growing in MPA-treated mice and from 60 tumors, were performed as previously described (Dran *et al*., 1995). In brief, tumors were aseptically removed, minced and washed with DMEM/F12 (Dulbecco's modified Eagle's medium/Ham's F12, 1 : 1, without phenol red, 100 U/ml penicillin and 100 μg/ml streptomycin). The tissue was suspended in 5 ml of enzymatic solution (trypsin: 2.5 mg/ml, albumin: 5 mg/ml and collagenase type II (Gibco – BRL, Gaithersburg, MD, USA): 239 U/ml) in phosphate buffered saline (PBS) and incubated at 37°C for 20 min, under continuous stirring. The liquid phase of the suspension was then removed and the undigested tissue was incubated with fresh enzymatic solution for 20 min. Enzyme action was stopped by adding DMEM/F12 + 5% heat inactivated fetal calf serum (FCS) (Gen SA, Buenos Aires). Epithelial and fibroblastic cells were separated as already described (Dran *et al*., 1995). Briefly, the cell suspension was resuspended in 15 ml of DMEM/F12 + 10% FCS and allowed to sediment for 20 min. The sedimented cells, corresponding to the epithelial enriched fraction, were resuspended again in 15 ml of DMEM/F12 + 5% FCS and allowed to sediment for other 20 min. The upper 15 ml were discarded and this procedure was repeated until no fibroblasts were observed in the supernatant. Cells were plated in culture flasks with DMEM/F12 + 5% steroid-stripped FCS (ChFCS) (Dran *et al*., 1995) and allowed to attach for 24 – 48 h. Purity of the epithelial cultures was evaluated by cytokeratin staining. Cells were incubated in DMEM/F12, (without phenol red, 100 U/ml penicillin and 100 μ/ml streptomycin), with 2.5% ChFCS in the presence or absence of MPA. After a 24 h incubation, 50% of media was replaced by fresh media and cells were incubated for another 24 h in the presence of 0.8 μCi of [^{3}H]-thymidine (NEN, Dupont, Boston MA, USA; specific activity: 70 – 90 Ci/mmol). Cells were then trypsinized and harvested. Assays were performed in octuplicate. The differences between control and experimental groups were analysed by ANOVA followed by Tukey *t*-test between groups. In former experiments we demonstrated that thymidine uptake correlates with the number of cells/well (Dran *et al*., 1995). MCF-7 cells were obtained from American Type Culture Collection. For experimental purposes MCF-7 cells were cultured in DMEM/F12 (without phenol red) supplemented with 0.1% ChFCS and HRG (20 ng/ml) or IGF-I (50 ng/ml).

Antisense studies

ErbB-2 antisense (5′-GGC CGC CAG CTC CAT) and sense (5′-ATG GAG CTG GCG GCC) oligodeoxynucleotides (ODNs) correspond to the translation start region, including the initiation codon of the ErbB-2 mRNA (Colomer *et al*., 1994). Type I IGF-R antisense (5′-TCC TCC GGA GCC A-GA CTT) and sense (5′-AAG TCT GGC TCC GGA GGA) ODNs correspond to codons 21 – 26 of the signal sequence of the subunit of type I IGF-R preceding the proreceptor sequence. ODNs were purchased from Nuclei Co (Buenos Aires, Argentina). The effect of ODNs was studied as follows: 0.2 ml/well of a cell suspension were seeded at a concentration of 10^5 cell/ml in a Falcon 96-well microtitreplate. After attachment (24 – 48 h), the cells were incubated for 48 h with medium (serum used in antisense studies was heated at 65 °C for 30 min to inactivate exonucleases) containing the indicated concentrations of ODNs. The media were changed every 24 h adding fresh ODNs. After incubation, [^{3}H]-thymidine was added and incorporation was determined as described above.

RTKs type-I and -II Western blotting

In order to study expression of RTKs, lysates were prepared from tumors growing in MPA-treated and -untreated mice and from primary cultures of C4HD or 60 cells. Tumors or cells were lysed in buffer containing 50 mM Tris (pH 7.4), 150 mM NaCl, 1 mM EDTA, 1 mM ethylene glycol-bis (β-aminoethyl ether)-N-N-N′-N′ tetraacetic acid (EGTA), 10% glycerol, 0.5% Nonidet P-40, 1 mM $ClMg_2$, 1 mM phenylmethylsulfonylfluoride (PMSF), 10 μg/ml leupeptin, 5 μg/ml pepstatin, 5 μg/ml aprotinin, 1 mM sodium orthovanadate, 5 mM NaF, 20 mM sodium molybdate and 5 mM sodium pyrophosphate. Lysates were centrifuged at 40 000 *g* for 40 min at 4°C and protein content in the supernatant was determined using a Bio-Rad kit (Richmond, CA, USA). Proteins were solubilized in sample buffer (60 mM Tris-HCl, pH 6.8, 2% SDS, 10% glycerol and 0.01% bromophenol blue) and subjected to SDS – PAGE on a 6% gel. Proteins were electroblotted on to nitrocellulose. Membranes were blocked with PBS, 0.1% Tween 20 (PBST) and immunoblotted with the following antibodies: ErbB-2 rabbit polyclonal antibody Neu C-18 (Santa Cruz Biotechnology, Santa Cruz, CA, USA), ErbB-3 rabbit polyclonal antibody C-17 (Santa Cruz Biotechnology), ErbB-4 rabbit polyclonal antibody C-18 (Santa Cruz Biotechnology), ErbB-4/HER-4 Oncoprotein Ab-2 rabbit polyclonal antibody (Neomarkers, Freemont, CA, USA), and IGF-IR β subunit mouse monoclonal antibody Ab-5 (clone 1-2) (Neomarkers). After washing, the membranes were incubated with HRP-conjugated secondary antibody (Amersham International, UK). Enhanced chemiluminescence (ECL) was performed according to manufacturer's instructions (Amersham).

To study the effects of ASODNs to ErbB-2 and to IGF-IR mRNAs on protein expression, lysates were prepared as described above from cells both treated and untreated with ODNs. Rabbit polyclonal anti-HRG antibody, specific for HRG precursor (C-20, Santa Cruz Biotechnology) was used in HRG studies.

RTKs tyrosine phosphorylation analysis

Lysates from tumors growing in MPA-treated and -untreated mice, from cells growing in 2.5% ChFCS, or cells treated for 48 h with 10 nM MPA or with the indicated ASODNs were prepared as decribed above. The amounts of protein immunoprecipitated from tumors growing in MPA-treated and untreated animals and from HI tumors were different (ranging from 0.5 – 1.5 mg), in order to correct for the MPA-induced increase in ErbB-2 and ErbB-3 levels and for the higher ErbBs expression in HI tumors. All lysates were precleared with Protein A-Agarose (Santa Cruz Biotechnology) and 2 – 5 μg of ErbB-2 Neu C-18, ErbB-3 C-17, and mouse monoclonal Anti-P-Tyr PY-99 antibodies (Santa Cruz Biotechnology) were used. Immunoprecipitations were rocked 2 h at 4°C and then the immunocomplexes were captured by adding Protein A-Agarose and rocked by an additional 2 h. Beads were washed three times with lysis buffer, then boiled for 10 min in sample buffer and subjected to SDS – PAGE on a 6% gel. Proteins were electroblotted on to nitrocellulose. Membranes were blocked with PBS, 0.1% Tween 20 (PBST), 5% bovine serum albumin (Sigma) and 1% ovoalbumin (Sigma) and filters were probed with mouse monoclonal

Anti-P-Tyr PY-99 (Santa Cruz Biotechnology) antibody when immunoprecipitations were performed with anti-ErbB-2 and anti-ErbB-3 antibodies or were probed with the IGF-IR β subunit mouse monoclonal antibody when immunoprecipitation was performed with the phosphotyrosine antibody PY-99. Proteins were visualized with HRP-conjugated secondary antibody, using ECL detection (Amersham). In experiments in which the tyrosine phosphorylation levels of ErbB-2 and ErbB-3 were studied, identical aliquots of each immunoprecipitate were subjected to immunoblot analysis with anti-ErbB-2 or anti-ErbB-3 antibodies to verify that nearly equal amount of proteins immunoprecipitated were loaded.

ErbB-2 and IGF-IR association

Whole lysates from tumors or primary cultures of C4HD and 60 cells or from MCF-7 cells were obtained as described above. Membrane preparations from tumors were obtained as previously reported (Elizalde *et al*., 1998). DTT 1 mM was added to the lysis buffer in experiments in which reducing conditions were used. One mg protein was immunoprecipitated with the ErbB-2 antibody as described. Immunoprecipitates were separated by SDS–PAGE and transferred to nitrocellulose. Filters were probed with either the IGF-IR β subunit mouse monoclonal antibody Ab-5 (clone 1–2) (Neomarkers) or the IGF-IR α subunit rabbit polyclonal antibody N-20 (Santa Cruz). When the immunoprecipitation-immunoblotting procedure was reversed, whole lysates or membrane preparations were immunoprecipitated with an anti-IGF-IR α chain antibody (Santa Cruz 2C8), and Western blotting was performed with the anti-ErbB-2 antibody. Anti-cyclin D1 was the mouse monoclonal antibody 72-13G (Santa Cruz), anti- TGF-βIIR was the rabbit polyclonal antibody L-21 (Santa Cruz) and ErbB-2 blocking peptide was obtained from Santa Cruz.

IGF-I receptor binding assay

Recombinant human IGF-I, kindly provided by Dr James Merryweather (Chiron, Emeryville, CA, USA), was iodinated and purified as described (Elizalde *et al*., 1998). Binding to intact cell monolayers from C4-HD epithelial cells treated with ODNs to IGF-IR was performed as described (Elizalde *et al*., 1998). Assays were performed in triplicate and results were analysed by the Scatchard method (1949).

Immunofluorescence staining and confocal microscopy

C4HD cells grown on glass coverslips were incubated in 2.5% ChFCS in the presence and absence of MPA 10 nM for 48 h. Cells were fixed in 2% paraformaldehide in PBS, pH 7.4 for 20 min at 4°C, washed in PBS and permeabilized for 7 min in 0.1% Triton X-100 in PBS. Cells were then blocked using PBS containing 1% BSA for 1 h at room temperature. ErbB-2 was localized using the ErbB-2 rabbit polyclonal antibody C-18 (Santa Cruz) and IGF-IR using the mouse monoclonal IGF-IR (Clone αIR3, Oncogene, Cambridge MA). Both antibodies were incubated for 1 h at room temperature. Following washing cells were incubated with with a rhodamine-conjugated anti-rabbit antibody (for ErbB-2) and with a fluorescein isothiocyanate-conjugated anti-mouse antibody (for IGF-IR) (Sigma). Stained cells were analysed using a Zeiss LSM 510 confocal laser scanning microscope. Negative control staining performed using isothiocyanate-conjugated and rhodamine-conjugated antibodies without incubation with primary antibodies showed no immunofluorescence signal (data not shown).

Acknowledgments
The authors wish to thank Dr C Lanari for providing the experimental model, Dr T Santa Coloma, and M Bianchini for help and advice with the confocal microscopy, and Dr E Bal de Kier Joffé for critical discussion and review of the manuscript. This work was supported by grants from the National Scientific Council of Argentina (CONICET) PID 4188/96, from the National Agency of Scientific Promotion of Argentina IDB 802/OC-AR PICT 0503402 and from the Centro Argentino Brasilero de Biotecnología (CABBIO).

References

Backer JM, Myers MG, Sun XJ, Chen DJ, Schoelson SE, Mivalpeix M and White MF. (1993). *J. Biol. Chem.,* **268,** 8204–8212.
Balañá ME, Lupu R, Labriola L, Charreau EH and Elizalde PV. (1999). *Oncogene,* **18,** 6370–6379.
Baserga R. (1995). *Cancer Res.,* **55,** 249–252.
Braunsberg H, Coldham NG, Learke RE, Cowan SK and Wong W. (1987). *Eur. J. Cancer Clin. Oncol.,* **23,** 563–571.
Carraway KL and Cantley LC. (1994). *Cell,* **78,** 5–8.
Clarke CL and Sutherland RL. (1990). *Endocr. Rev.,* **11,** 266–302.
Cohen GB, Ren R and Baltimore D. (1995). *Cell,* **80,** 237–248.
Colomer R, Lupu R, Bacus SS and Gelmann EP. (1994). *Br. J. Cancer,* **70,** 819–825.
Coppola D, Ferber A, Masahiko M, Sell C, D'Ambrosio C, Rubin R and Baserga R. (1994). *Mol. Cell. Biol.,* **14,** 4588–4595.
Dati C, Antoniotti S, Taberna D, Perroteau I and De Bortoli M. (1990). *Oncogene,* **5,** 1001–1006.
De Bortoli M and Dati C. (1997). *J. Mam. Gland. Biol. Neoplasia,* **2,** 175–185.
Dickson R and Lippman ME. (1995). *Endocrin. Rev.,* **16,** 559–589.
Dran G, Luthy IA, Molinolo AA, Montecchia F, Charreau EH, Dosne Pasqualini C and Lanari C. (1995). *Breast Cancer Res. Treat.,* **35,** 173–186.
Egan SE and Weinberg RA. (1993). *Nature,* **365,** 781–783.
Elizalde PV, Lanari C, Bussman L, Kordon E, Guerra F, Savin M and Charreau EH. (1990). *J. Exp. Clin. Cancer Res.,* **9,** 193–203.
Elizalde PV, Lanari C, Molinolo AA, Guerra FK, Balañá ME, Simian M, Iribarren A and Charreau EH. (1998). *J. Steroid. Biochem. Molec. Biol.,* **67,** 305–317.
Fedi P, Pierce J, Di Fiore PP and Kraus M. (1994). *Mol. Cell. Biol.,* **14,** 492–500.
Graus-Porta D, Beerli RR, Daly JM and Hynes NE. (1997). *EMBO J.,* **16,** 1647–1655.
Groshong SD, Owen GI, Grimison B, Schauer IE, Todd MC, Langan TA, Sclafani RA, Lange C and Horwitz KB. (1997). *Mol. Endocrinol.,* **11,** 1593–1607.
Grunt TW, Saceda M, Martin MB, Lupu R, Dittrich E, Krupitza G, Harant H, Huber H and Dittrich C. (1995). *Int. J. Cancer,* **63,** 560–567.

Holmes WE, Sliwkowski MX, Akita RW, Henzel WJ, Lee J, Park JW, Yansura D, Abadi N, Raab H, Lewis GD, Shepard M, Wood WI, Goeddel DV and Vandlen RL. (1992). *Science,* **256,** 1205 – 1210.

Kavanaugh WM and Williams LT. (1994). *Science,* **266,** 1862 – 1865.

Kiss R, Paridaens RJ, Heuson JC and Danguy AJ. (1986). *J. Natl. Cancer Inst.,* **77,** 173 – 178.

Kordon EC, Guerra FK, Molinolo AA, Elizalde PV, Charreau EH, Dosne Pasqualini CD, Montecchia F, Pazos P, Dran G and Lanari C. (1994). *Int. J. Cancer,* **59,** 196 – 203.

Kraus MH, Issing W, Miki T, Popescu NC and Aaronson SA. (1989). *Proc. Natl. Acad. Sci. USA,* **86,** 9193 – 9197.

Lanari C, Kordon E, Molinolo AA, Dosne Pasqualini C and Charreau EH. (1989). *Int. J. Cancer,* **43,** 845 – 850.

Lange CA, Richer JK, Shen T and Horwitz K. (1998). *J. Biol. Chem.,* **273,** 31308 – 31316.

LeRoith D, Werner H, Beitner-Johnson D and Roberts CT. (1995). *Endocr. Rev.,* **16,** 143 – 163.

Lewis GD, Lofgren JA, McMurtrey AE, Nuijens A, Fendly BM, Bauer KD and Sliwkowski MX. (1996). *Cancer Res.,* **56,** 1457 – 1465.

Lowenstein EJ, Daly RJ, Batzer AG, Li W, Margolis B, Lammers R, Ullrich A, Skolnik EY, Bar-Sagi D, Schlessinger J. (1992). *Cell,* **70,** 431 – 442.

Lupu R and Lippman ME. (1993). *Breast Cancer Res. Treat.,* **27,** 83 – 93.

Manni A, Badger B, Wright C, Ahmed JR and Demers LM. (1987). *Cancer Res.,* **47,** 3066 – 3071.

Migliaccio A, Di Domenico M, Castoria G, de Falco A, Bontempo P, Nola E and Auricchio F. (1996). *EMBO J.,* **15,** 1292 – 1300.

Migliaccio A, Piccolo D, Castoria G, Di Domenico M, Bilancio A, Lombardi M, Gong W, Beato M and Auricchio F. (1998). *EMBO J.,* **17,** 2008 – 2018.

Ming XF, Burgering BMT, Wennstrom S, Claeson-Welsh L, Heldin C, Bos JL, Kozma SC and Thomas G. (1994). *Nature,* **371,** 426 – 429.

Modiano JF, Kokai Y, Weiner DB, Pykett MJ, Nowell PC and Lyttle CR. (1991). *J. Cell. Biochem.,* **45,** 196 – 206.

Molinolo AA, Lanari C, Charreau EH, San Juan N and Dosne Pasqualini C. (1987). *J. Natl. Cancer Inst.,* **79,** 1341 – 1350.

Murphy LJ, Surtherland RL, Stead B, Murphy LC and Lazarus L. (1986). *Cancer Res.,* **46,** 728 – 734.

Murphy LC, Murphy LJ, Dubik D, Bell GI and Shiu RP. (1988). *Cancer Res.,* **48,** 4555 – 4560.

Pelicci G, Lanfrancone N, Grignani F, McGlade J, Cavallo F, Forni G, Nicoletti I, Grignani F, Pawson T, Pelicci PG. (1992). *Cell,* **70,** 93 – 104.

Pinkas-Kramaski R, Alroy I and Yarden Y. (1997). *J. Mam. Gland. Biol. Neoplasia,* **2,** 97 – 107.

Plowman GD, Whitney GS, Neubauer MG, Green JM, McDonald VL, Todaro GJ and Shoyab M. (1990). *Proc. Natl. Acad. Sci. USA,* **87,** 4905 – 4909.

Plowman GD, Culouscou J-M, Whitney GS, Green JM, Carlton GW, Foy L, Neubauer MG and Shoyab M. (1993). *Proc. Natl. Acad. Sci. USA,* **90,** 1746 – 1750.

Ram TG, Kokeny KE, Dilts CA and Ethier SP. (1995). *J. Cell. Physiol.,* **163,** 589 – 596.

Ram TG, Dilts CA, Dziubinski ML, Pierce LJ and Ethier SP. (1996). *Mol. Carcinog.,* **15,** 227 – 238.

Read LD, Keith D, Slamon DJ and Katznellenbogen BS. (1990). *Cancer Res.,* **50,** 3947 – 3951.

Richer JK, Lange C, Manning NG, Owen G, Powell R and Horwitz KB. (1998). *J. Biol. Chem.,* **273,** 31317 – 31326.

Riese DJ II and Stern DF. (1998). *Bioessays,* **20,** 41 – 48.

Sarup JC, Rao KV and Fox CF. (1988). *Cancer Res.,* **48,** 5071 – 5078.

Scatchard G. (1949). *Ann. NY Acad. Sci.,* **51,** 660 – 672.

Stewart AJ, Johnson MD, May FEB and Westley BR. (1990). *J. Biol. Chem.,* **265,** 21172 – 21178.

Swantek JL and Baserga R. (1999). *Endocrinology,* **140,** 3163 – 3169.

Taverna D, Antoniotti S, Maggiora P, Dati C, De Bortoli M and Hynes NE. (1994). *Int. J. Cancer,* **56,** 522 – 528.

Tzahar E, Waterman H, Chen X, Levkowitz G, Karunagaran D, Lavi S, Ratzkin BJ and Yarden Y. (1996). *Mol. Cell. Biol.,* **16,** 5276 – 5287.

Ullrich A, Coussens L, Hayflick JS, Dull TJ, Gray A, Tam AW, Lee J, Yarden Y, Libermann TA, Schelessinger J, Downward J, Mayes ELV, Whittle N, Waterfield MD, Seeburh PH. (1984). *Nature,* **309,** 418 – 425.

Ullrich A, Gray A, Tam AW, Yan-Feng T, Tsubokawa M, Collins C, Hensel W, LeBon T, Kathuria S, Chen F, Jacobs S, Franke U, Ramachandran J and Fujita-Yamaguchi Y. (1986). *EMBO J.,* **5,** 2503 – 2512.

Van der Geer P, Hunter T and Lindberg RA. (1994). *Annu. Rev. Cell. Biol.,* **10,** 251 – 337.

Woods-Ignatoski KM, Lapointe AJ, Radany EH and Ethier SP. (1999). *Endocrinology,* **140,** 3615 – 3622.

Yamamoto T, Ikawa S and Akiyama T. (1986). *Nature,* **319,** 230 – 234.